Inorganica Chimica Acta, 198–200 (1992) 483–491

NMR is a unique and necessary step in the investigation of iron sulfur proteins: the HiPIP from *R. gelatinosus* as an example

Ivano Bertini*
University of Florence, Department of Chemistry, via G. Capponi 7, 50121 Florence (Italy)

Francesco Capozzi, Claudio Luchinat
University of Bologna, Institute of Agricultural Chemistry, viale Berti Pichat 10, 40127 Bologna (Italy)

Mario Piccioli and Margarita Vicens Oliver
University of Florence, Department of Chemistry, via G. Capponi 7, 50121 Florence (Italy)

Abstract

^{1}H NOE and 2D NMR studies have been performed on oxidized and reduced HiPIP from *Rhodocyclus gelatinosus* (formerly *Rhodopseudomonas gelatinosa*). By saturating the β-CH_2 protons of the cysteines in the oxidized form which are hyperfine shifted, NOEs are measured on signals which have been then assigned to specific residues through 2D NMR. In this way the signals of the cysteines have been specifically assigned. Since we had already related the shifts of the β-CH_2 protons to the oxidation state of each iron, we succeeded in connecting the individual cysteines with the oxidation state of each iron. Support for the assignment comes from 2D measurements of the reduced protein which is less paramagnetic. Signals in the oxidized and reduced species can be related through EXSY. These results represent a unique and successful strategy to frame an iron sulfur cluster within a protein, with the iron ions labelled according to their oxidation number.

Introduction

The iron sulfur clusters in proteins contain iron ions in different oxidation states, which are bound to cysteines and to inorganic sulfur [1, 2]. The investigation through X-ray spectroscopy does not yet distinguish between iron in the oxidation state +2 from that in the oxidation state +3 when both are present in the same cluster. The approach to the characterization of the iron ions has to be spectroscopic. Mössbauer spectroscopy is of fundamental importance in detecting the oxidation state, whereas magnetic Mössbauer provides information on the hyperfine coupling between ^{57}Fe and the unpaired electron on that iron ion [3, 4]. This information can be related to the electronic structure of the cluster as it results from magnetic coupling between the iron ions [3–6]. Similar information is obtained from the hyperfine coupling with nuclei of the ligands studied through NMR spectroscopy [7–12]. In this case the temperature dependence of the hyperfine coupling is also an important feature.

The final step in the investigation of these systems is that of recognizing which cysteine is bound to a certain iron ion with electronic structure already characterized. This step can be accomplished only by NMR [13, 14]. From this technique we know that a certain proton senses an iron in a given oxidation state. This proton will be close to other protein residues. The point is that of recognizing to which residue it is close through NOE and 2D NMR. Then the proton is assigned to a certain cysteine. The difficulty is that of revealing NOE and 2D connectivities in paramagnetic systems [15]. We are now learning how to overcome at least partially these difficulties.

High potential iron sulfur proteins (HiPIP hereafter) are four-iron four-sulfur proteins which in the reduced form contain two Fe^{2+} and two Fe^{3+} ions. From Mössbauer and NMR we know that in the reduced form iron is in the oxidation state 2.5, whereas in the oxidized state there are two iron(III) and two iron in the 2.5 oxidation state.

We succeeded in determining which cysteine is bound to each type of iron in the case of HiPIP from *Chromatium vinosum* for which the X-ray structure is known [16, 17]. We would like to perform the same type of assignment in the case of *Rhodocyclus gelatinosus* (formerly *Rhodopseudomonas gelatinosa*) for which the X-ray structure is not known. Despite the homology of

*Author to whom correspondence should be addressed.

0020-1693/92/$5.00

R. gelatinosus and *C. vinosum* being low (less than 40%), it is likely that the overall tertiary structure is similar [18]. If so, the residue homology around the cluster is relatively high. Another goal of this research is thus to find experimental evidence to support or disprove this hypothesis.

Experimental

All chemicals used were of the best quality available. HiPIP was isolated from *R. gelatinosus* following the procedure reported by Bartsch [19]. Protein purity was checked through UV–Vis spectroscopy.

Sample deuteration was performed by solvent exchange utilizing an ultrafiltration Amicon cell, equipped with a YM5 membrane.

All the ^{1}H NMR data were recorded on an AMX spectrometer operating at 600 MHz Proton Larmor Frequency. All the experiments were performed at 300 K unless specified. ^{1}H NMR spectra were performed using a presaturation pulse to suppress the solvent signal. Typically 512 scans were collected over 16 384 data points. Recycle delay was 500 ms. ^{1}H NOE experiments were performed using the superWEFT pulse sequence (180–τ–90–AQ) [20]. Saturated signals were selectively irradiated for about 150 ms during the τ delay of the sequence. Recycle delay was about 200 ms. The difference spectra were obtained using a previously reported methodology [21].

NOESY [22] and TOCSY [23] experiments were performed in the time proportional phase incrementation mode. In the oxidized form both NOESY and TOCSY spectra over the diamagnetic signal region were collected using about 30 ms of mixing time. 2K×1K data points were collected over about 15 000 Hz of spectral window. Squared shifted sine bell weighting functions were applied in both dimensions. NOESY experiments in the reduced state were performed using 5 ms of mixing time and 80 ms of relaxation delay. 1K×256 data point matrix was acquired over about 25 000 Hz of spectral window. In order to detect connectivities involving fast relaxing signals a 512×256 data point matrix has been transformed. Squared shifted sine bell weighting functions have been applied in both dimensions.

COSY experiments on the reduced form of the enzyme were collected in magnitude mode [24]. 1K×512 data point matrix was acquired over 25 000 Hz of spectral window. 100 ms of relaxation delay was used. In order to obtain information on fast relaxing signals, only a 200×100 data point matrix was used. Zero filling and squared sine bell weighting functions were applied in both dimensions.

Strategies

(i) We will start with the analysis of the 1D NOE difference spectra obtained by selectively saturating the nine far shifted resonances in the oxidized state.

(ii) The signals showing NOEs in the diamagnetic part of the spectrum will be investigated in the NOESY and TOCSY maps. This step will allow us to assign some specific residues.

(iii) The 1D NOE difference spectra will be compared with those obtained upon saturation of β-CH_2 protons of the iron coordinated cysteines of oxidized HiPIP from *C. vinosum* [13]. The analogies between the two series of spectra will be helpful for the specific assignment of β-CH_2 proton pairs.

(iv) An extensive series of 2D experiments on the reduced state of the protein will confirm the assignment of the four β-CH_2 protons, already obtained through EXSY experiments [9], and will provide independent evidences for the assignment of at least two of the four β-CH_2 proton pairs. Since saturation transfer experiments among the two oxidation states has been already performed [9], information obtained on different oxidation states are confirmative.

(v) On these bases the sequence specific assignment of the four cysteines bound to iron ions will be performed, and the structure around the cluster will be compared with that previously reported for *C. vinosum* HiPIP [16, 17].

Results and discussion

The 600 MHz NMR spectra of *R. gelatinosus* HiPIP in the reduced and oxidized state are reported in Fig. 1(a) and (b). In the reduced state (Fig. 1(a)), four hyperfine shifted resonances can be easily identified from 18 to 10 ppm downfield, which show an anti-Curie temperature dependence. They are assigned to four of the eight β-CH_2 of iron coordinated cysteines. In the oxidized state (Fig. 1(b)) nine resonance experience a sizable isotropic shift. NOE and saturation transfer experiments have allowed the pairwise assignment of all the resonances to coordinated cysteine β-CH_2 protons [9] in both oxidation states. Connectivities reported in Fig. 1 show the corresponding signals in the oxidized and reduced states. Signal E′ was tentatively proposed to be the Hα proton of the cysteine whose β-CH_2 resonances are C′ and D′ [9].

The experimental approach has been outlined in the description of the strategies used for the assignment. On that basis we have been able to perform the sequence specific assignment or iron coordinated cysteine residues. Table 1 reports the chemical shifts of β-CH_2 and α-CH of cysteines in both oxidized and reduced state.

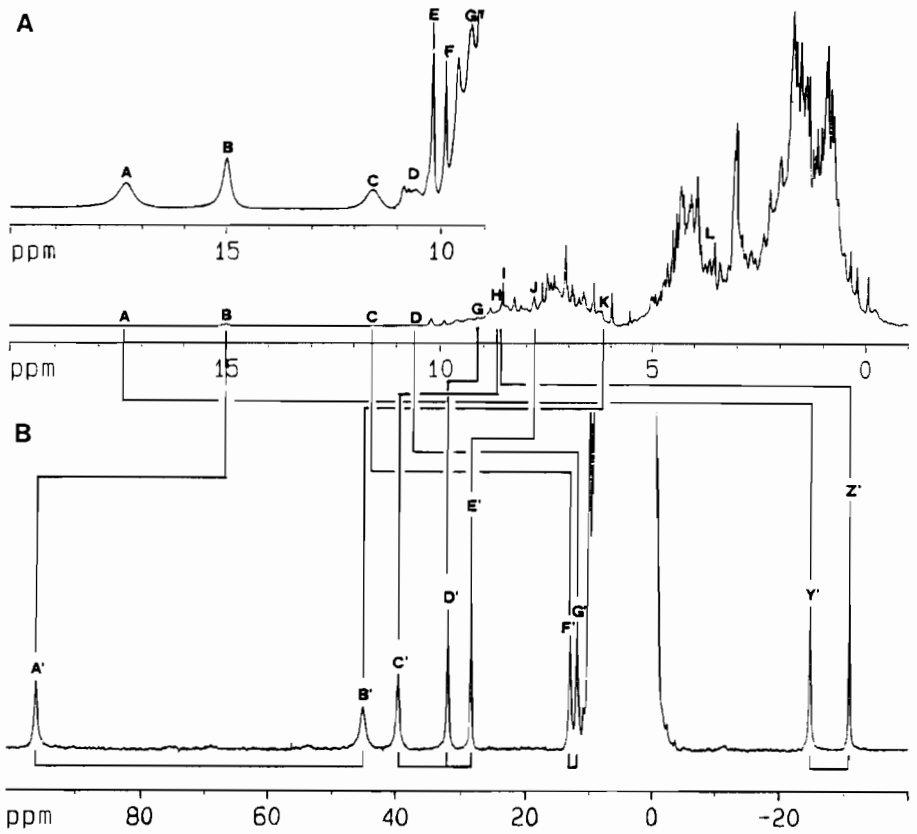

Fig. 1. 600 MHz, 300 K, ^{1}H NMR spectra of reduced (A) and oxidized (B) HiPIP from *R. gelatinosus* in D_2O at pH* 7.2 and 5.1, respectively. The region between 20 and 9 ppm of the reduced state is vertically expanded in the inset. Signals are labelled according to previously published labelling [9]. Lines indicate connectivities among signals, observed through NOE and saturation transfer experiments [9].

TABLE 1. Assignment of cysteine protons in reduced and oxidized HiPIP from *R. gelatinosus*

Assignment	Reduced		Oxidized	
	Signal	$\delta^{a,b}$	Signal	$\delta^{a,c}$
Cysteine 43 Hβ1	I	8.63	Z′	−30.88
Cysteine 43 Hβ2	A	17.33	Y′	−24.83
Cysteine 43 Hα			10	2.73
Cysteine 46 Hβ1	D	10.6	G′	11.83
Cysteine 46 Hβ2	C	11.5	F′	12.94
Cysteine 46 Hα				
Cysteine 63 Hβ1	K	6.12	B′	45.08
Cysteine 63 Hβ2	B	14.98	A′	95.78
Cysteine 63 Hα	L	3.69		
Cysteine 77 Hβ1	G	9.35	D′	31.93
Cysteine 77 Hβ2	H	8.70	C′	39.51
Cysteine 77 Hα	J	7.8	E′	28.39

[a]Chemical shifts are expressed in ppm. They have been obtained at 300 K. [b]pH* = 7.2. [c]pH* = 5.1.

For ease of comparison, throughout this article, the numbering of residues follows that of *C. vinosum* [18].

Oxidized HiPIP

Figure 2 shows the 1D NOE difference spectra obtained upon saturation of isotropically shifted resonances in the oxidized state. The NOEs which have been used for the assignment are labelled with numbers and their assignment is reported in Table 2. Basically, all the inter residue distances which have been crucial for the assignment of cysteine protons of *C. vinosum* HiPIP [13], are observed also in the case of *R. gelatinosus*.

The assignment of signals A′ and B′ to Cys 63 is based on the NOE to an aromatic residue (signal 1 in Fig. 2), to two CH_3 groups which, from TOCSY and NOESY, are assigned to a valine residue (signals 4 and 5 in Fig. 2) and on saturation transfer experiments which allow Cys 63 β-CH_2 protons to be assigned in the reduced state (see later). Figure 3 shows that signals 4 and 5 belong to a spin system characteristic of a valine residue. In *C. vinosum* there are no valine residues whose methyl groups can give NOE upon saturation of β-CH_2 protons (Table 3). However, in *R. gelatinosus*, there is a valine substituting one of the above residues, namely Ile 71. Indeed, γ-CH_3 of Ile 71 in *C. vinosum* experiences NOE from Hβ_2 of Cys 63 [13]. We can thus use NOE data to predict the reciprocal orientation

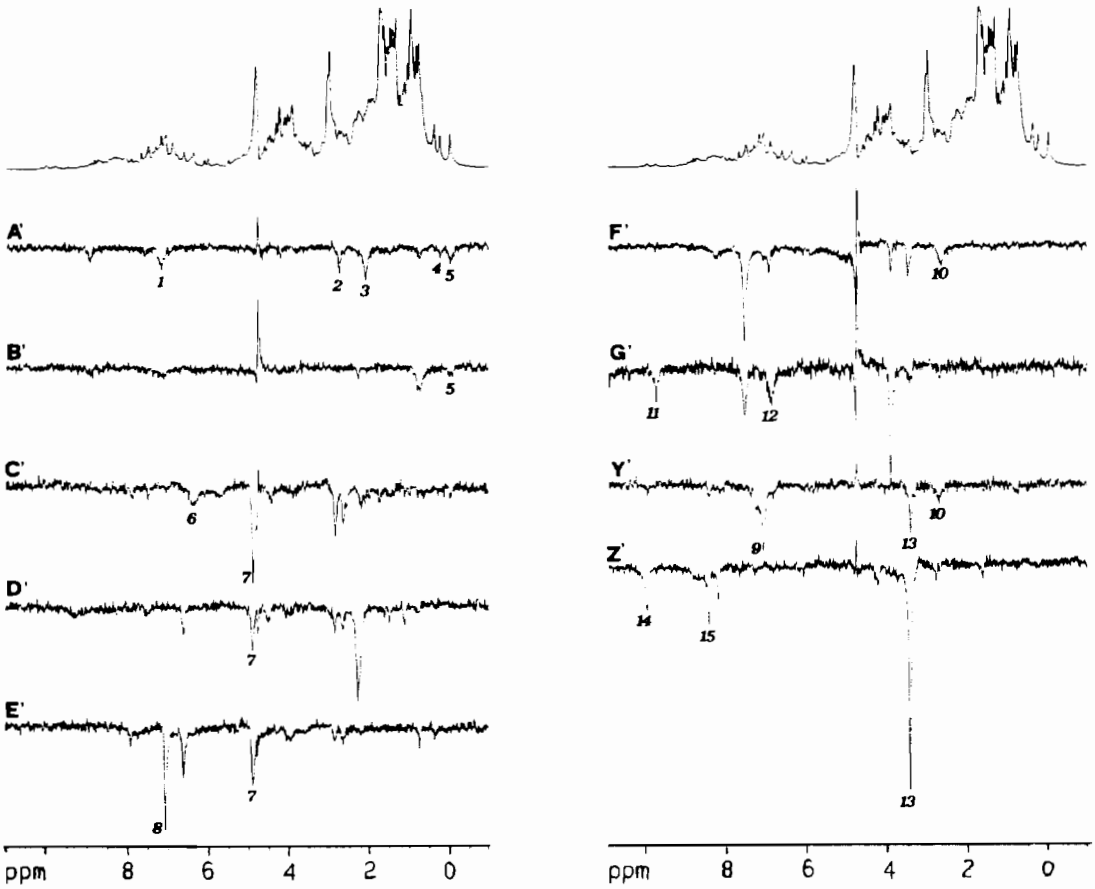

Fig. 2. 600 MHz, 300 K, ^{1}H NOE difference spectra of oxidized HiPIP from *R. gelatinosus* in D_2O at pH*5.1 obtained upon saturation of isotropically shifted signals A′ to Z′. Traces are labelled on the basis of the saturated signals. Labelling of the observed NOEs follows the assignment reported in Table 2. The difference spectra are scaled in such a way that the areas of the irradiated signals (not shown) are all equal.

of Val 71 and Cys 63. The X-ray structure of *C. vinosum* HiPIP shows also that the aromatic signal (signal 1 in Fig. 2) has to be the *ortho* proton of Phe 66, which is conserved in *R. gelatinosus* (Table 3). The full pattern of Phe 66 does not appear in the TOCSY spectrum since the T_1 values are too short. However, the reduced protein allows the Phe 66 residue from the NOESY spectrum to be assigned (see later).

From the X-ray structure of *C. vinosum* HiPIP we note that Tyr 19, which is also conserved in *R. gelatinosus* (Table 3), is at a very short distance from Cys 77. Tyr 19 Hα proton is at short distances from all of the three Cys 77 protons; this feature is unique and allows us to assign resonances C′, D′ and E′ as belonging to the Cys 77 residue since they all give strong NOE with signal 7 (Fig. 2).

The NOE from signal G′ to the NH proton of a Trp residue (signal 11 in Fig. 2) makes firm the assignment of F′ and G′ β-CH_2 protons to Cys 46. Indeed, Cys-46 Hβ_1 in *C. vinosum* is the only proton, among the four cysteine residues, which is close to a Trp residue (Trp 80, which is conserved in *R. gelatinosus*), in such a way to give NOE to both the ring NH and the Hδ_1 protons [13]. G′ gives also NOE to a signal at 6.92 ppm (signal 12 in Fig. 2), and there is a NOESY cross peak between signal 11 and 12 (data not shown) allowing us to assign signal 12 as the Hδ_1 proton of Trp 80. An interesting structural feature of the Fe_4S_4 HiPIP from *C. vinosum* is provided by the short inter residue distance between Cys 43 Hα and Cys 46 Hβ_2 [16, 17]. Due to the short distances occurring between Cys 43 Hα and the iron ions of the cluster, the Cys 43 Hα resonance is broad and hardly detectable [13]. We have been able to observe the connectivity between Cys 43 Hα and Cys 46 Hβ_2 in *C. vinosum* [13] and we have also been able to observe it in *R. gelatinosus* (signal 10 in Fig. 2 in both traces F′ and Y′). Obviously, this provides a further important element for the assignment. Signal Y′ and Z′ are thus assigned to Cys 43.

As far as Cys 43 is concerned, it is worth noting that a strong dipolar connectivity has been detected from Hβ_2 to an aromatic residue (signal 9 in Fig. 2). Since no aromatic signals were detected upon saturation

TABLE 2. Dipolar connectivities observed upon saturation of isotropically shifted signals of oxidized *R. gelatinosus* and their assignment

Irradiated signal	Responding signal	Assignment
A′	1	Hδ Phe 66[a]
A′	2	$H\beta_2$ Phe 66[a,b]
A′	3	$H\beta_1$ Phe 66[a,b]
A′	4	$\gamma_1(\gamma_2)CH_3$ Val 71[a,b]
A′	5	$\gamma_2(\gamma_1)CH_3$ Val 71[a,b]
B′	5	$\gamma_2(\gamma_1)CH_3$ Val 71[a,b]
C′	6	Hδ Tyr 19[a]
C′	7	Hα Tyr 19[c]
D′	7	Hα Tyr 19[c]
E′	8	$H\epsilon_3$ Trp 76[d]
E′	7	Hα Tyr 19[c]
F′	9	Hδ Phe 49[c]
F′	10	Hα Cys 43[c]
G′	11	NH Trp 80[a]
G′	12	Hδ1 Trp 80[a]
Y′	9	Hδ Phe 49[c]
Y′	13	Hα Asn 73[c]
Y′	10	Hα Cys 43[c]
Z′	14	NH Cys 43(Ala 44)[d]
Z′	15	NH Ala 44(Cys 43)[d]
Z′	13	Hα Asn 73[c]

[a]Assigned from NOESY experiments. [b]Assigned from TOCSY experiments. [c]Assigned from NOEs obtained upon saturation of cysteine protons. [d]Tentitatively assigned by comparison with X-ray data and previously performed experiments on *C. vinosum* HiPIP.

of the Cys 43 $H\beta_2$ resonance in the case of *C. vinosum* HiPIP, we assign signal 9 to a proton of Phe 49 which in *R. gelatinosus* replaces Met 49 (Table 3). The full TOCSY pattern of this Phe residue appears in the reduced protein. The observation of a dipolar connectivity with $H\beta_2$ of Cys 43 can help in defining the position of Phe 49 inside the cavity.

Comparison of NOEs on the two proteins in the oxidized state shows some differences in the aliphatic region for Cys 43 and Cys 63 β-CH_2 resonances. This is consistent with the Ile 71 → Val 71 and Met 49 → Phe 49 substitutions occurring close to Cys 63 and Cys 43, respectively. The NOE (signal 9) in the aromatic region upon saturation of Cys 43 suggests that Phe 49 is oriented toward Cys 43. This seems to be a situation similar to that observed in the recently solved X-ray structure of *Ectothiorhodospira halophila* HiPIP I at 2.5 Å resolution, in which Met 49 is replaced by a triptophane which is located at a short distance from Cys 43 [25].

Although no residue is changed around Cys 77, some structural difference is detected between *C. vinosum* and *R. gelatinosus*. This appears from several independent evidences.

(i) The intra residue NOEs on Cys 77 Hα, obtained upon saturation of both βCH_2 protons, are changed. While in the case of *C. vinosum* HiPIP, NOEs of 9% and 4% were observed to peak E′ upon saturation of Cys 77 Hβ1 and Hβ2, respectively, in the case of *R. gelatinosus* the NOEs observed to peak E′ are 4.6 and 4.8%, respectively.

(ii) Among the two βCH_2 protons, the more downfield shifted is the broader one, at variance with what was observed in the case of *C. vinosum* HiPIP.

(iii) Comparison of the patterns of NOEs in the difference spectra obtained upon saturation of Cys 77 βCH_2 protons in the oxidized state suggests that the assignment of signals C′ and D′ is reversed with respect to *C. vinosum*.

(iv) In the reduced state, the Cys 77 $H\beta_1$ proton undergoes a sizeable decrease in chemical shift, compared with that observed for *C. vinosum* (9.35 versus 12.77 ppm). This feature is unique for Cys 77, the other cysteine βCH_2 proton signals being very similar in the two derivatives.

On these bases we can state that, for *R. gelatinosus*, some modest geometrical changes with respect to *C. vinosum* have occurred at the Cys 77 site. The NOE

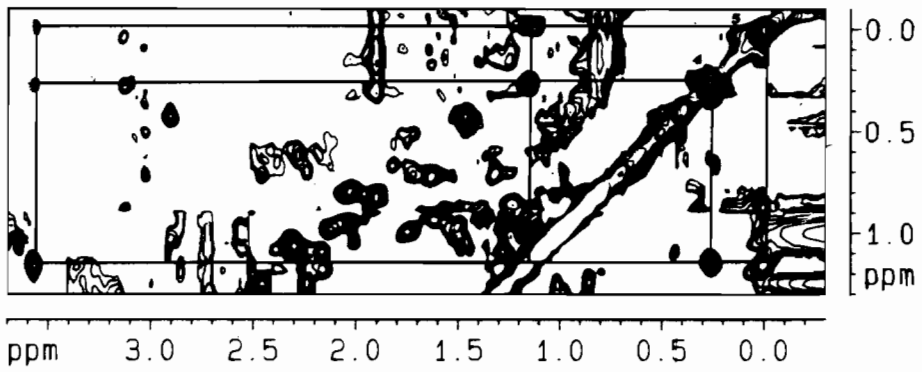

Fig. 3. 600 MHz, 300 K, ^1H NMR TOCSY experiment (section in the aliphatic region) on oxidized HiPIP from *R. gelatinosus* in D_2O at pH*5.1 An MLEV 17 [23] spin lock field has been applied for 40 ms. Lines show connectivities of the spin system of a valine residue.

TABLE 3. Shortest proton–proton distances from cysteine protons from the X-ray structure of *Chromatium vinosum* HiPIP

	Distance (Å)	Amino acid residue in *R. gelatinosus* HiPIP
Cysteine 43 Hβ1		
Hα Val 73	2.51	replaced by Asn
NH Cys 43	2.68	conserved
NH Ala 44	2.91	replaced by Gly
NH Gly 75	2.92	conserved
Hα Cys 43	3.00	conserved
CH_3 Ile 71	3.52, 3.99, 4.28	replaced by Val
Hγ Met 49	3.98	replaced by Phe
Cysteine 43 Hβ2		
$CH_3\delta$ Ile 71	2.39, 2.80, 3.78	replaced by Val
Hα Cys 43	2.45	conserved
Hγ1 Met 49	2.90	replaced by Phe
Hα Val 73	3.54	replaced by Asn
NH Cys 43	3.64	conserved
Hβ1 Met 49	3.80	replaced by Phe
Hγ2 Met 49	3.83	replaced by Phe
NH Ala 44	3.89	replaced by Gly
Hβ1 Cys 46	3.92	conserved
Cysteine 46 Hβ1		
Hα Cys 46	2.29	conserved
Hδ1 Trp 80	2.50	conserved
NHε1 Trp 80	2.93	conserved
Hα Cys 43	2.93	conserved
NH Thr 81	3.45	conserved
Hα Trp 80	3.76	conserved
Cysteine 46 Hβ2		
Hβ1 Met 49	2.63	replaced by Phe
Hα Cys 43	2.71	conserved
Hα Cys 46	2.97	conserved
NH Met 49	3.53	replaced by Phe
Hβ1 Cys 43	3.93	replaced by Phe
Cysteine 63 Hβ1		
$H\gamma_1$ Ile 71	1.88	replaced by Val
Hα Cys 63	2.52	conserved
$H\gamma_2$ Ile 71	2.86	replaced by Val
γCH_3 Ile 71	3.03, 3.94, 4.73	replaced by Val
$H\delta_1$ Phe 66	3.13	conserved
$H\beta_1$ Phe 66	3.39	conserved
NH Cys 63	3.45	conserved
δCH_3 Ile 71	3.55, 4.37, 4.56	replaced by Val
Cysteine 63 Hβ2		
$H\beta_1$ Phe 66	1.76	conserved
$H\delta_1$ Phe 66	2.23	conserved
NH Phe 66	2.79	conserved
NH Cys 63	3.00	conserved
Hα Cys 63	3.06	conserved
$H\gamma_1$ Ile 71	3.38	replaced by Val
γCH_3 Ile 71	3.45, 4.08, 5.12	replaced by Val
$H\beta_2$ Phe 66	3.50	conserved
$H\gamma_2$ Ile 71	3.99	replaced by Val
Cysteine 77 Hβ1		
$H\beta_1$ Tyr 19	2.09	conserved
Hα Cys 77	2.20	conserved
$H\beta_1$ Leu 17	2.30	conserved
Hα Tyr 19	2.60	conserved
NH Tyr 19	3.33	conserved
$H\beta_2$ Leu 17	3.36	conserved
$H\beta_2$ Tyr 19	3.49	conserved
$H\delta_1$ Tyr 19	3.60	conserved
δ_1CH_3 Leu 17	3.65, 4.84, 5.34	conserved
Cysteine 77 Hβ2		
Hβ1 Tyr 19	2.01	conserved
Hδ1 Tyr 19	2.05	conserved
Hα Cys 77	2.51	conserved
Hα Tyr 19	2.64	conserved
NH Cys 77	3.18	conserved
Hβ2 Tyr 19	3.76	conserved
Hβ2 Leu 17	3.78	conserved
NH Tyr 19	3.91	conserved

data are indicative of a change in the β–C–C–α dihedral angles and β–α distances. A variation of 20° in the β–C–C–α dihedral angles, in the direction of bringing the α proton closer to the plane bisecting the β_1–β_2 angle, would rationalize this finding. Such a variation in the structures of the two HiPIPs would provide a variation in the Hβ–Fe distances not greater than 10%. Hence these observations lead us to assign signal D′ as Cys 77 Hβ1 and signal C′ as Cys 77 Hβ2, i.e. in the reverse shift order with respect to *C. vinosum* HiPIP. The NOE extent from Cys 77 protons and Tyr 19 Hα for *C. vinosum* also supports the proposed assignment.

Reduced HiPIP

The characterization of the reduced state provides further independent evidences for the assignment. The reduced protein is less paramagnetic, in the case of *C. vinosum*, μ_{eff} being 0.84 μ_B per iron versus 1.84 μ_B per iron in the oxidized species [26]. Therefore 2D experiments are more readily performed. Figure 4 reports parts of a NOESY spectrum showing the connectivities involving the isotropically shifted resonances. Besides the four $H\beta_1$–$H\beta_2$ connectivities (A/I, B/K, C/D and G/H), signal A shows a cross peak at 7.32 (A/a), unobserved in the case of *C. vinosum* reduced HiPIP. This signal is assigned to a ring proton of Phe 49, also clearly observed in the oxidized state upon saturation of Y′.

Signal B, besides the intra residue connectivities (B/K and B/L), also observed in the COSY experiment reported in Fig. 5(A), gives two strong cross peaks at 7.41 (B/b) and 2.25 ppm (B/c). From the pattern of

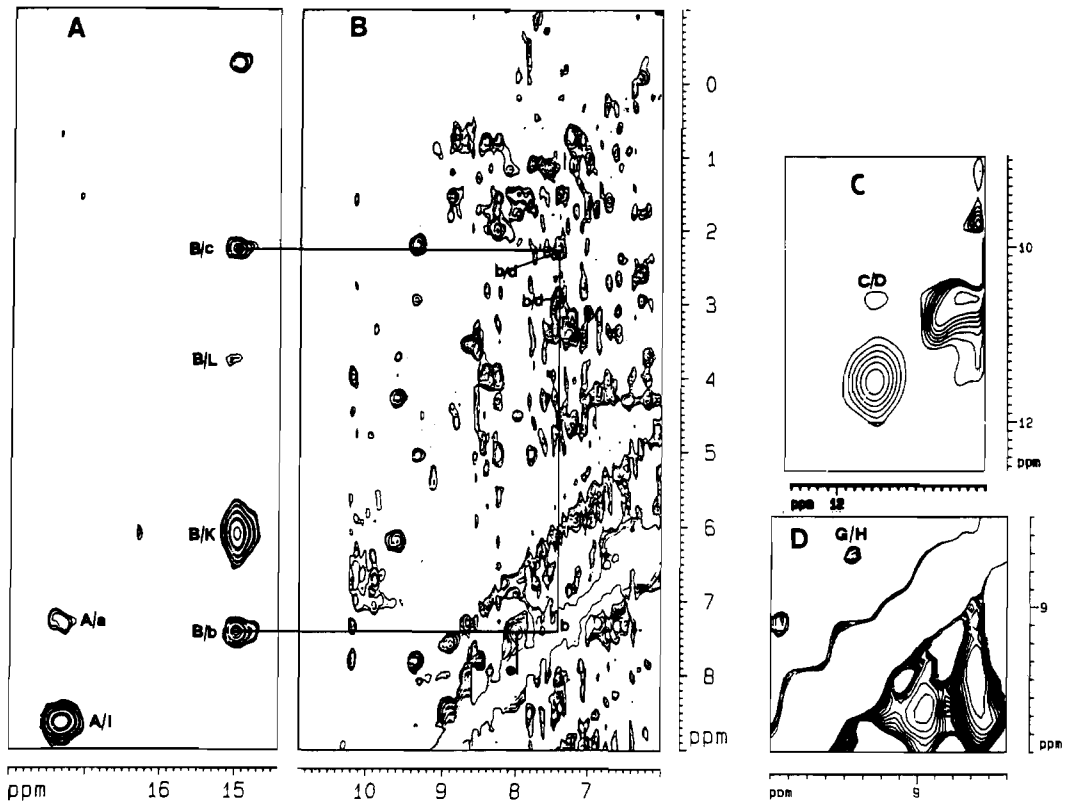

Fig. 4. 600 MHz, 300 K, ^{1}H NMR NOESY spectrum of reduced HiPIP from *R. gelatinosus* in D_2O at pH*7.2. Spectrum has been recorded using 5 ms of mixing time and relaxation delay of 80 ms. Several regions of the same spectrum are reported. They have been obtained using different data processing. Region A reports connectivities involving isotropically shifted signals. Region B reports connectivities among signal B and Phe 66 residue. Regions C and D report connectivities between the less isotropically shifted β-CH_2 cysteine protons.

dipolar connectivities shown in Fig. 4(B), supported also by COSY and TOCSY experiments (data not shown), signals b, c, d and e can be assigned to the Phe 66 residue (Hδ, Hβ_2, Hβ_1 and Hϵ, respectively).

Figure 5(A) shows the COSY spectrum of the reduced state in the spectral region of the more isotropically shifted β-CH_2 cysteine protons. It is worth noting that the relative extent of NOESY and COSY cross peaks between Cys 63 β and α protons is analogous to what was observed in the case of *C. vinosum* HiPIP [13].

Figure 5(B) reports the TOCSY spectrum of the spectral region in which aromatic residues are expected to be detected. In the reduced state, one triptophane (W) and two phenylalanines (F) can be identified. The observed NOESY connectivity A/a of Fig. 4(A) leads us to assign the phenylalanine residue with signals at 7.41, 7.37 and 7.33 ppm as Phe 49.

Structural inferences

The NOEs from β-CH_2 protons of Cys 63 to Val 71 are not consistent with the reciprocal orientation of Cys 63 and Ile 71 as it appears from *C. vinosum* data [16, 17]. In essence, Hβ_2 of Cys 63, which should be farther from Val 71, gives stronger NOEs with both γCH_3 groups than Hβ_1. There are no conceivable movements of the Val residue which can reverse the NOE patterns. On the other hand, a variation of about 30° in the β–C–C–α dihedral angles of Cys 63 would yield interproton distances consistent with the NOE data. The proposed variation of the structure with respect to crystallographic data on *C. vinosum* would be also more consistent with the observed NOE extent from Cys 63 Hβ_2 to Phe 66 Hβ_2, which is weaker than expected. Interestingly, such a variation would make the Fe–S–C–H dihedral angles, φ, more consistent with the observed chemical shift of Cys 63 β-CH_2 protons in the assumption of a $\sin^2\varphi$ dependence of the isotropic shift [13].

Among the other cysteine residues, we have already pointed out that a variation of about 20° in dihedral angles of Cys 77 from *C. vinosum* to *R. gelatinosus* would account for the experimental data. In this case, no other structural differences occur between the two proteins and NOE from Cys 77 to Tyr 19 indicates no major differences in the disposition of neighboring residues. As a consequence, this structural variation

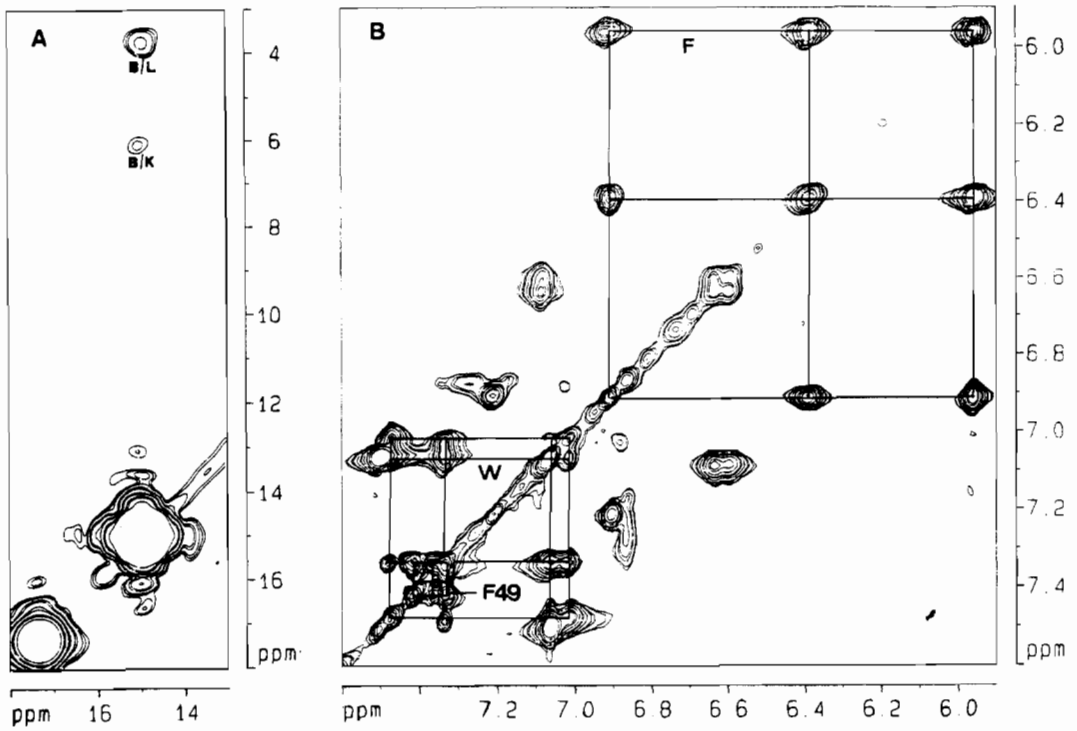

Fig. 5. 600 MHz, 300 K, ^{1}H NMR COSY (A) and TOCSY (B) spectra of reduced HiPIP from *R. gelatinosus* in D_2O at pH*7.2. Spectrum A reports scalar connectivities involving the more isotropically shifted signals. Spectrum B shows scalar connectivities detected inside the region of aromatic resonances, observed through TOCSY spectroscopy.

seems to be simply due to a different geometrical disposition of Cys 77 itself.

We have also discussed that Met 49 is replaced by Phe 49 in the case of *R gelatinosus*. Since Met 49 in the structure of *C. vinosum* is in the proximity of the cluster we may expect one more aromatic residue around the cluster on passing form *C. vinosum* to *R. gelatinosus*. Indeed, NOEs from signal Y′ to signal 9 in the oxidized state (Fig. 2), and from signal A to signal a in the reduced state (Fig. 4(A)) confirm this prediction. These NOEs allow us to predict the position of Phe 49 inside the protein. The six membered ring of phenylalanine seems to be close to the Cys 43 residue. In particular, the distance between Hβ_2 Cys 43 and Hδ Phe 49 should be about 3.0 Å. Indeed, comparison with the recently solved X-ray structure of HiPIP from *E. halophila I* [25], in which position 49 is occupied by a Trp residue, suggests that Phe 49 of *R. gelatinosus* is placed in the same position as Trp 49 in *E. halophila I*, the two aromatic residues being almost coplanar.

The above structural elements constitute a picture that, although rough, can be considered the first step on the route to the elucidation of the solution structure of a paramagnetic metalloprotein.

Electronic features and individual oxidation states

As outlined in the 'introduction', the peculiar signs and temperature dependences of the isotropic shifts of the β-CH_2 protons in oxidized HiPIPs have been accounted for on the ground of a simple exchange coupling model [7, 9]. In this model, which is based on evidence from Mössbauer spectra, the signals which are shifted upfield, or those which are shifted downfield but with an anti-Curie temperature dependence, belong to cysteines coordinated to iron(III) ions, whereas the signals shifted downfield but with a Curie-type temperature dependence belong to the mixed-valence iron(II)–iron(III) pair. The results of the present investigation clearly show that, as in *C. vinosum* HiPIP [13, 14], the two iron(III) ions are bound to cysteines 43 and 46, whereas the iron ions constituting the mixed-valence pair are bound to cysteines 63 and 77.

Owing to the remarkable similarity of the arrangement of amino acid residues around the cluster, we can conclude that the overall tertiary structure is maintained. As in the case of *C. vinosum* HiPIP, the only edge of the cluster accessible from outside of the protein is likely to be the inorganic sulfur ion bridging Fe 46, Fe 63 and Fe 77. This feature may be important for the electron transfer pathway in these systems.

Acknowledgements

Thanks are expressed to J. W. Carter and to H. M. Holden for providing us with the X-ray coordinates of

the reduced form of *C. vinosum* HiPIP and of *E. halophila* HiPIP I, respectively.

References

1 W. Lovenberg (ed.), *Iron Sulfur Proteins*, Vols. 1 and 2, Academic Press, New York, 1973.
2 T. G. Spiro (ed.), *Iron-Sulfur Proteins*, Vol. 4, Wiley–Interscience, New York, 1982.
3 P. Middleton, D. P. E. Dickson, C. E. Johnson and J. D. Rush, *Eur. J. Biochem., 104* (1980) 289.
4 D. P. E. Dickson, C. E. Johnson, R. Cammack, M. C. W. Evans, D. O. Hall and K. K. Rao, *Biochem. J., 139* (1974) 105.
5 (a) V. Papaefthymiou, J.-J. Girerd, I. Moura, J. J. G. Moura and E. Munck, *J. Am. Chem. Soc., 109* (1987) 4703; (b) E. Munck, V. Papaefthymiou, K. K. Surerus and J.-J. Girerd, in L. Que (ed.), *Metal Clusters in Proteins*, ACS Symposium Series, American Chemical Society, Washington, DC, 1988.
6 L. Noodleman, *Inorg. Chem., 26* (1988) 3677.
7 I. Bertini, F. Briganti, C. Luchinat, A. Scozzafava and M. Sola, *J. Am. Chem. Soc., 113* (1991) 1237; *113* (1991) 7084.
8 L. Banci, I. Bertini, F. Briganti, C. Luchinat, A. Scozzafava and M. Vicens Oliver, *Inorg. Chim. Acta, 180* (1991) 171.
9 L. Banci, I. Bertini, F. Briganti, C. Luchinat, A. Scozzafava and M. Vicens Oliver, *Inorg. Chem., 30* (1991) 4517.
10 L. Banci, I. Bertini and C. Luchinat, *Struct. Bonding (Berlin), 72* (1990) 113.
11 L. Banci, I. Bertini, F. Briganti and C. Luchinat, *New J. Chem., 15* (1991) 467.
12 I. Bertini and C. Luchinat, *NMR of Paramagnetic Molecules in Biological Systems*, Benjamin/Cummings, Menlo Park, CA, 1986.
13 I. Bertini, F. Capozzi, S. Ciurli, C. Luchinat, L. Messori and M. Piccioli, *J. Am. Chem. Soc., 114* (1992) 3332.
14 D. G. Nettesheim, S. R. Handen, B. A. Feimberg and J. D. Otvos, *Biochemistry, 31* (1992) 1234.
15 (a) L. Banci, I. Bertini, C. Luchinat and M. Piccioli, in I. Bertini, H. Molinari and N. Niccolai (eds.), *NMR and Biomolecular Structure*, VCH, Weinheim, 1991; (b) I. Bertini, F. Capozzi, C. Luchinat and P. Turano, *J. Magn. Reson., 95* (1991) 244.
16 C. W. Carter Jr., J. Kraut, S. Freer, Ng. H. Xuong, R. A. Alden and R. G. Bartsch, *J. Biol. Chem., 249* (1974) 4212.
17 C. W. Carter Jr., J. Kraut, S. T. Freer and R. A. Alden, *J. Biol. Chem., 249* (1974) 6339.
18 C. T. Przysiecki, T. E. Meyer and M. A Cusanovich, *Biochemistry, 24* (1985) 2542.
19 R. G. Bartsch, *Methods Enzymol., 53* (1978) 329.
20 T. Inubushi and E. D. Becker, *J. Magn. Reson., 51* (1983) 128.
21 L. Banci, I. Bertini, C. Luchinat, M. Piccioli, P. Turano and A. Scozzafava, *Inorg. Chem., 28* (1989) 4650.
22 S. R. Macura and R. R. Ernst, *Mol. Phys., 40* (1980) 95.
23 D. G. Davis and A. Bax, *J. Magn. Reson., 65* (1985) 355.
24 A. Bax, R. Freeman and G. Morris, *J. Magn. Reson., 42* (1981) 164.
25 D. R. Breiter, T. E. Meyer, I. Rayment and H. M. Holden, *J. Biol. Chem., 266* (1991) 18660.
26 W. D. Phillips, C. C. MacDonald, N. A. Stombaugh and W. H. Orme-Johnson, *Proc. Natl. Acad. Sci. U.S.A., 71* (1974) 140.